Redox-sensing by PecS from the plant pathogen

Pectobacterium atrosepticum and its effect on gene
expression and the conformation of PecS-bound

promoter DNA

Dinesh K. Deochand[#], Anuja Pande[†], Jacob K. Meariman[‡], Anne Grove*

Department of Biological Sciences, Louisiana State University, Baton Rouge, LA 70803, USA

Running title: PecS oxidation affects gene expression and DNA conformation

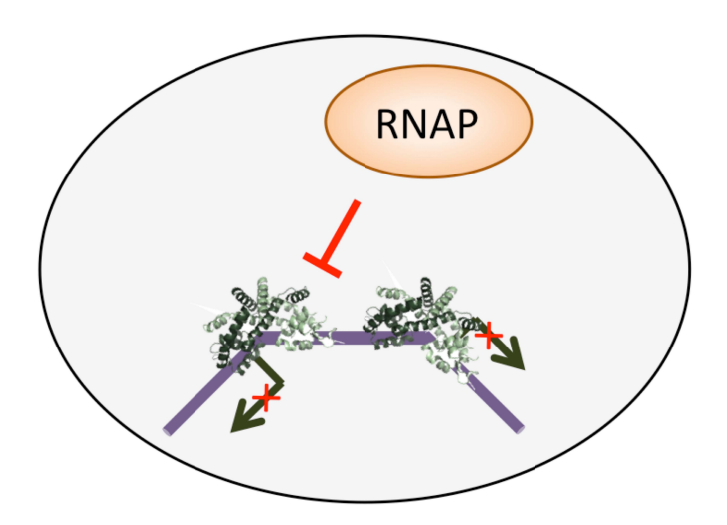
Present addresses: *Hospital for Special Surgery and Weill Cornell Medical College, New York, NY; †Department of Immunology and Microbiology, University of Colorado School of Medicine, Aurora, CO; *Louisiana State University Health Sciences Center, New Orleans, LA *To whom correspondence should be addressed: Anne Grove, Department of Biological Sciences, Louisiana State University, Baton Rouge, LA 70803. Tel: 225-578-5148. Email: agrove@lsu.edu

Keywords: Gene regulation; transcription factor; reactive oxygen species; DNase I footprinting; MarR; cysteine oxidation; DNA distortion

ABSTRACT

The plant pathogen Pectobacterium atrosepticum encounters a stressful environment when it colonizes the plant apoplast. Chief among the stressors are the reactive oxygen species (ROS) that are produced by the host as a first line of defense. Bacterial transcription factors in turn use these signals as cues to upregulate expression of virulence-associated genes. We have previously shown that the transcription factor PecS from P. atrosepticum binds the promoters that drive expression of pecS and pecM, which encodes an efflux pump, to repress gene expression. We show here that addition of oxidant relieves repression in vivo and in vitro. While reduced PecS distorts promoter DNA on binding, oxidized PecS does not, as evidenced by DNaseI footprinting. PecS oxidation is reversible, as shown by an oxidant-dependent quenching of intrinsic tryptophan fluorescence that is completely reversed on addition of reducing agent. Cysteine 45 positioned at the PecS dimer interface is the redox-sensor; reduced PecS-C45A causes less DNA distortion on binding compared to wild-type PecS, addition of oxidant has no effect on binding, and PecS-C45A cannot repress gene expression. Our data suggest that reduced PecS distorts its cognate DNA on binding, perhaps inducing a conformation in which promoter elements are suboptimally aligned for RNA polymerase binding, resulting in transcriptional repression. In contrast, oxidized PecS binds promoter DNA such that RNA polymerase may successfully compete with PecS for binding, allowing gene expression. This mode of regulation would facilitate induction of the PecS regulon when the bacteria encounter host-derived ROS in the plant apoplast.

For Table of Contents Use Only



Introduction

Reactive oxygen species (ROS) are generated as by-products of aerobic metabolism. An excess of such species can damage cellular components, including proteins, nucleic acids, and lipids, a condition referred-to as oxidative stress.¹ For those reasons, ROS are also generated during the defenses mounted by an organism, be it plant or animal, in response to an invading pathogen.² However, pathogenic bacteria exploit these signals as cues to induce their own response to the host defenses. Upon sensing ROS, bacterial cells activate the expression of genes involved in neutralization of oxidative free radicals and genes encoding repair systems; this response is often controlled by transcription factors that can directly sense the presence of ROS or metabolites associated with ROS production.^{3,4}

Bacterial transcription factors belonging to the MarR (Multiple Antibiotic Resistance Regulators) family have been implicated in gene regulation in response to oxidative stress and in regulation of genes that encode virulence factors. Typically, these transcription factors mediate regulatory function by binding to the shared operator/promoter regions of *marR* and a gene oriented divergently from the *marR* gene as well as to other genes in their regulons. MarR proteins either repress or activate expression of their target genes, a regulatory function that is modulated in presence of small molecule ligands or redox-active compounds.⁵

PecS, a MarR family transcription factor, is a master regulator of virulence gene expression in the enterobacterium *Dickeya dadantii*, a causative agent of soft-rot disease in a variety of plant species.^{6,7} *D. dadantii* PecS controls a number of virulence genes, including genes encoding degradative enzymes such as pectinases. It also represses expression of the divergent *pecS* and *pecM* genes; PecM is an efflux pump through which the antioxidant indigoidine is exported, and failure to export indigoidine attenuates virulence, demonstrating the importance of an efficient

antioxidant response.⁸ The signal to which *D. dadantii* PecS responds to regulate gene activity has not been reported.

Repression of divergent *pecS-pecM* genes by PecS has also been demonstrated in *Klebsiella pneumoniae*, *Agrobacterium fabrum*, *Streptomyces coelicolor*, *Vibrio vulnificus*, and in the phytopathogen *Pectobacterium atrosepticum*, which causes soft-rot and black-leg disease in potato. ⁹⁻¹³ In all these cases, urate (and in some cases xanthine as well) was shown to bind PecS, as a result of which DNA binding was attenuated and *pecS-pecM* expression was increased. Urate and xanthine are generated by plant xanthine dehydrogenase, which contributes to ROS formation when the host mounts a defense against a bacterial infection; urate in addition functions to prevent oxidative damage to plant cells. ^{14,15} Mammalian xanthine oxidase is likewise involved in ROS production in response to infection, with the attendant accumulation of urate. ¹⁶ Invading bacteria may therefore sense accumulation of these purine metabolites to augment their own defense and promote host colonization.

Soft-rot phytopathogens such as *D. dadantii* and *P. atrosepticum* colonize the plant apoplast, where they encounter mildly acidic pH (pH 5-6.5), nutrient limitation, and plant-derived ROS, among other environmental signals.¹⁷ The bacteria alkalinize the apoplast by producing acetoin, which raises the pH to ~8, the pH at which pectinases have their optimal activity.¹⁸ We recently reported that *P. atrosepticum* PecS responds to pH by altering its mode of DNA binding;¹² at neutral pH, PecS distorts DNA and represses the *pecS* promoter, while mildly alkaline pH (pH~8) leads to deprotonation of a specific histidine, causing significant attenuation of DNA distortion (but not binding affinity) and derepression of gene activity. This suggests that while PecS proteins may respond to a common inducing ligand, they may have evolved to respond to additional signals to optimize function.

We show here that *P. atrosepticum* PecS also directly senses oxidative stress, which has not been previously reported for PecS proteins. Oxidation of a specific cysteine that is situated at the PecS dimer interface attenuates the DNA distortion that is imposed by reduced protein, and addition of oxidant leads to derepression of gene activity *in vivo*. We propose that *P. atrosepticum* PecS modulates gene expression by altering core promoter topology in response to ROS and that it has evolved to sense multiple signaling cues to mediate differential gene expression most effectively.

Materials and Methods

Purification of PecS and mutant proteins

PecS (originally cloned from *P. atrosepticum* SCRI 1043; *ECA_RS10035*) was purified after overexpression in *E. coli* Bl21(DE3)pLysS with an N-terminal His₆-tag as previously described.¹² The PecS mutants were constructed by whole-plasmid PCR using the recombinant plasmid harboring the *P. atrosepticum pecS* gene as a template. Cys45 was substituted with Ala using primers C45A-Fwd 5'-CTCAGGCGAGCAGCTGTGCTTATGGATCAGCGTCTGGA-3' and C45A-Rev 5'-AAGCACAGCACGTCGCCTGAGGCGTCCAATCG-3' whereas Cys81 was replaced with Ala using C81A-Fwd 5'-GCACCGCATGCTCTTAGTCCGACCGAACTCTTC-3' and C81A-rev 5'-CGGACTAAGTCGATGCGTGCACCTGCAC-3' (mutated codons boldfaced). The PCR products were transformed into *E. coli* Top10 cells after digestion with DpnI, and integrity of the variants was verified by DNA sequencing. Both mutant proteins were overexpressed in *E. coli* BL21(DE3)pLysS and purified as described for wild type PecS.¹² The purity was confirmed by SDS-PAGE gel electrophoresis and the concentration estimated by Micro BCA Protein Assay Kit (Pierce) using bovine serum albumin (BSA) as standard.

To investigate the effect of oxidizing agents on the oligomeric state of PecS proteins, 15 μ M reduced protein was incubated with different concentration of hydrogen peroxide (10 μ M, 50 μ M, 100 μ M, 500 μ M, and 1 mM), cumene hydroperoxide (CHP), and tertiary butyl hydroperoxide (TBP) for 15 minutes at 4 °C. The air-oxidized protein and reduced protein were used as controls. The reversibility of disulfide bond formation was assessed by addition of 20 mM β -mercaptoethanol to oxidized proteins. Samples were then analyzed by SDS-PAGE and the gels stained with Coomassie Brilliant Blue.

Thermal shift assay

For determination of thermal stability, proteins (10 μM) were diluted in TSA buffer (50 mM Tris-HCl pH 7.4, 100 mM NaCl, and 5X SYPRO Orange dye (Invitrogen)). Fluorescence emission induced by binding of the dye to the hydrophobic core of unfolded protein was measured at a temperature range of 2-90 °C in one-degree increment on an Applied Biosystems 7500 Real-Time PCR instrument (SYBR green filter). To assess the effect of oxidizing agent on thermal stability, PecS protein was incubated with different concentrations of hydrogen peroxide or CHP prior to thermal stability measurement. The total florescence intensity measured was corrected for buffer contributing to the signal and data were analyzed using Sigma Plot 9 by fitting the sigmoidal part of melting curve to a four-parameter sigmoidal equation. The T_m values are the average from three independent experiments (±SD) each determined from three technical replicates.

Intrinsic fluorescence measurement

A Jasco FP-6300 spectrofluorimeter was used to record the fluorescence emission spectra from 280 nm to 440 nm after exciting protein samples at 280 nm. PecS (10 μM) was added to FL buffer (40 mM Tris-HCl pH 7.4, 0.2 mM EDTA, 0.1% Brij58, 100 mM NaCl, and 10 mM

MgCl₂) in a 0.5 cm path-length cuvette. To oxidize the protein, H₂O₂ was added at various concentrations to the reaction mixtures, which were then incubated for 15 min. To assess reversibility of oxidation, protein was first equilibrated with oxidizing agent and then dithiothreitol (DTT) was added to reduce the protein. The fluorescence spectra were plotted using KaleidaGraph 4.0 after correcting observed fluorescence profile for dilution.

DNA binding

Electrophoretic mobility shift assay (EMSA) was performed to assess the DNA binding of PecS and the effect of oxidant. The 92-bp (*pecO*) sequence containing the *pecS-pecM* intergenic region was amplified and labeled with ³²P at the 5′-end using T4 polynucleotide kinase. EMSA was performed as previously described. ¹² To determine the effect of oxidation, PecS (2.5 nM) was incubated with increasing concentration of H₂O₂ or CHP for 15 min and then mixed with 0.1 nM ³²P-labeled *pecO* in a binding buffer (50 mM Tris (pH 7.4), 200 mM NaCl, 0.05% Brij58, 20 μg/mL BSA, and 4% glycerol). Complex and free DNA was separated by electrophoresis on 8% non-denaturing gels and complex formation analyzed by phosphorimaging software (ImageQuant 1.1).

DNase I footprinting

The DNase I footprinting was performed as reported.²⁰ Briefly, binding reactions containing 30 ng (14 nM) 6-FAM (6-carboxyfluorescein)-labeled 317 bp DNA probe including the *pecS-pecM* intergenic region were incubated for 15 min with or without reduced protein (28 nM) in binding buffer (50 mM Tris (pH 7.4), 200 mM NaCl, 0.05% Brij58, 20 μg/mL BSA, and 4 % glycerol), followed by DNase I digestion. The DNA fragment used for footprinting was longer than the one

used for EMSA since signal from the ends of the DNase I-digested fragment is lost due to sample processing and injection artifacts and to ensure the existence of unprotected DNA flanking the footprint. For analysis of effect of oxidation, proteins were treated with 2 mM H₂O₂ prior to incubation with DNA. The digested DNA was extracted by phenol-chloroform-isoamyl alcohol (25:24:1) and ethanol precipitated and dissolved in 10 μl Hi-Di formamide. Digested DNA was diluted in 10 μl formamide to a final concentration of 0.2 ng/mL and 1 μl of 1:10 diluted LIZ-500 size standard (Applied Biosystems) was added. DNA fragments were analyzed using an ABI 3130 automated capillary sequence analyzer. All electropherograms were processed using GeneMapper 4.1 software. Hypersensitive cleavage was quantitated by adding the intensity of identified hypersensitive sites and normalizing against the sum of an equivalent number of peaks whose intensity did not change on protein addition. The extent of cleavage was then normalized to DNase I-digested DNA to which no PecS was added; data are presented as the average of at least three independent experiments (with standard deviations).

Fluorescence microscopy

The gene encoding d1EGFP, which is a destabilized version of enhanced green fluorescent protein that reduces *in vivo* half-life, was expressed under control of the *pecS* promoter (*pecO*) in plasmid pACYC184.¹² The pACYC184_EGFP_*pecO* construct and expression vector harboring the relevant *pecS* gene variant were co-transformed into *E. coli* Bl21(DE3). Cells were grown in LB containing 30 μ g/mL chloramphenicol and 100 μ g/mL ampicillin at 37 °C to OD₆₀₀ of 0.5-0.6 with or without IPTG (0.3 mM). For analysis of the effect of oxidant, cells were treated with 250 μ M H₂O₂ at OD₆₀₀ ~0.3 and again exposed to H₂O₂ (250 μ M) after 15 min. The cells were harvested by centrifugation and resuspended in fresh LB medium at OD ~1.0. About 5 mL of

culture was deposited on a glass slide and observed using DIC (Differential Interference Contrast) and fluorescence microscopy. Images were acquired using a Leica DM6B-Z deconvolution microscope with 63X, 1.40-numerical aperture oil immersion objective lens. A GFP filter with excitation range 480/40 and emission range 527/30 was used for recording EGFP fluorescence. Images were captured by a Hamamatsu-Flash4-CL camera 16-bit with exposure time of 1 s. Phase contrast and fluorescence images were processed using Leica application suite X (LAS X). Representative examples of at least three experiments are shown.

In vitro transcription

To mimic the divergently oriented pecS-pecM gene pair, a DNA template was created in which mTagBFP2 (codon-optimized sequence synthesized with flanking NruI and KasI sites) was ligated to the pACYC184_EGFP_pecO construct such that EGFP is under control of the pecS promoter and mTagBFP2 is downstream of the pecM promoter. The final construct (pACYC184_EGFP_pecO_mTagBFP2) was verified by sequencing. A 294 bp DNA containing the entire intergenic region and extending 144 bp upstream into the coding region of EGFP1 and 67 bp downstream into the coding region of mTagBFP2 was amplified by PCR using the final 5′construct DNA template with forward primer Invitro-Fw GATGAACTTCAGGGTCAGCTTGCCGTAGGTG-3' and reverse primer Invitro-Rev 5'-CGGTGCCCTCCATGTACAGCTTCATGT-3'. Transcription was initiated as follows: 25 nM of the PCR-amplified DNA (EGFP_pecO_mTagBFP2) fragment was incubated with reduced or oxidized dimeric protein at different molar ratios (protein:DNA) for 30 min at room temperature in binding buffer (50 mM Tris (pH 7.4), 200 mM NaCl, 0.05% Brij58, 20 µg/mL BSA, and 4% glycerol) followed by addition of NTPs (0.25 mM each of ATP, CTP, and GTP, 0.01 mM UTP,

and 0.5 μCi α -³²P-UTP), 1X *E. coli* RNAP reaction buffer, and 0.05 U of *E. coli* RNAP holoenzyme (New England Biolabs). Reaction mixtures were incubated at 37 °C for 35 min. The reactions were terminated by addition of 10 mM EDTA and 73 bp ³²P-labelled DNA fragment was added as recovery marker prior to sample processing. Transcripts were purified by phenol-chloroform extraction and subjected to electrophoresis on 5% denaturing polyacrylamide gels. The resultant run-off transcripts were quantified by phosphorimaging software (ImageQuant 1.1). Experiments were performed in triplicate.

Results

Potential redox-active cysteines in P. atrosepticum PecS

P. atrosepticum PecS is a member of the urate-responsive subfamily of MarR proteins. Like other members of this family, PecS responds to urate by a mechanism involving attenuation of DNA binding. P. atrosepticum PecS negatively auto-regulates its own expression and that of the divergently oriented pecM gene by binding two sites in the pecS-pecM intergenic region at neutral pH (Fig. 1A), and urate induces gene expression in vivo. This genomic locus is conserved in a number of phytopathogens belonging to the gamma-proteobacterial family Enterobacteriaceae (including D. dadantii and P. atrosepticum), in the alpha-proteobacterial family Rhizobiaceae (e.g., A. fabrum), and in Streptomycetaceae (e.g., S. coelicolor). In D. dadantii, PecM is implicated in efflux of the antioxidant indigoidine, which is required to prevent oxidative stress imposed by the plant defense.

Although *P. atrosepticum* PecS shares significant sequence homology with other PecS homologs, it contains three cysteine residues per monomer (C45, C56, and C81), which is atypical for PecS proteins (Fig. 2). To map the position of cysteine residues in PecS, a three-

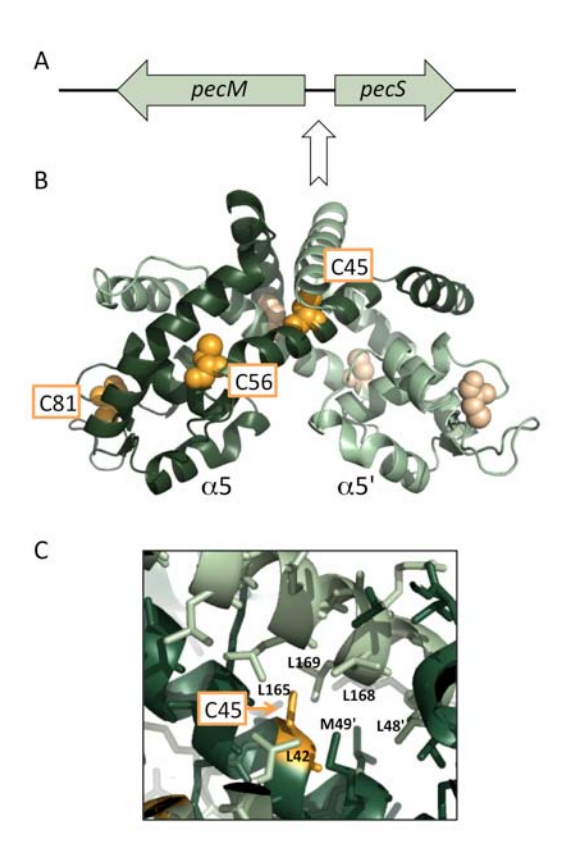


Figure 1. A. Genomic locus illustrating divergent pecS and pecM genes. The 63 bp intergenic region contains two 18 bp palindromic sequences identified as sites for PecS binding, each a few bp upstream of the respective start codons.¹² B. Model of *P. atrosepticum* PecS (GMQE 0.59) based on template 5DD8 (HucR-E48Q; 31% identity), a urate-responsive MarR variant from *Deinococcus radiodurans*.²³ Model was generated in SwissModel in automated mode and illustrated using PyMol. One monomer is in dark green with identified cysteines in yellow; the other subunit is in pale green with cysteines in pale yellow. Recognition helices (α 5/ α 5') are identified. C. Cys45 is predicted to reside in a pocket lined by hydrophobic residues.

dimensional model was generated. The model suggests that C45 is located at the pivot point of the long $\alpha 2$ helices that form the scaffold for the dimer interface, facing a hydrophobic pocket lined mainly with leucine residues, C56 is near the C-terminus of $\alpha 2$, and C81 is in the loop

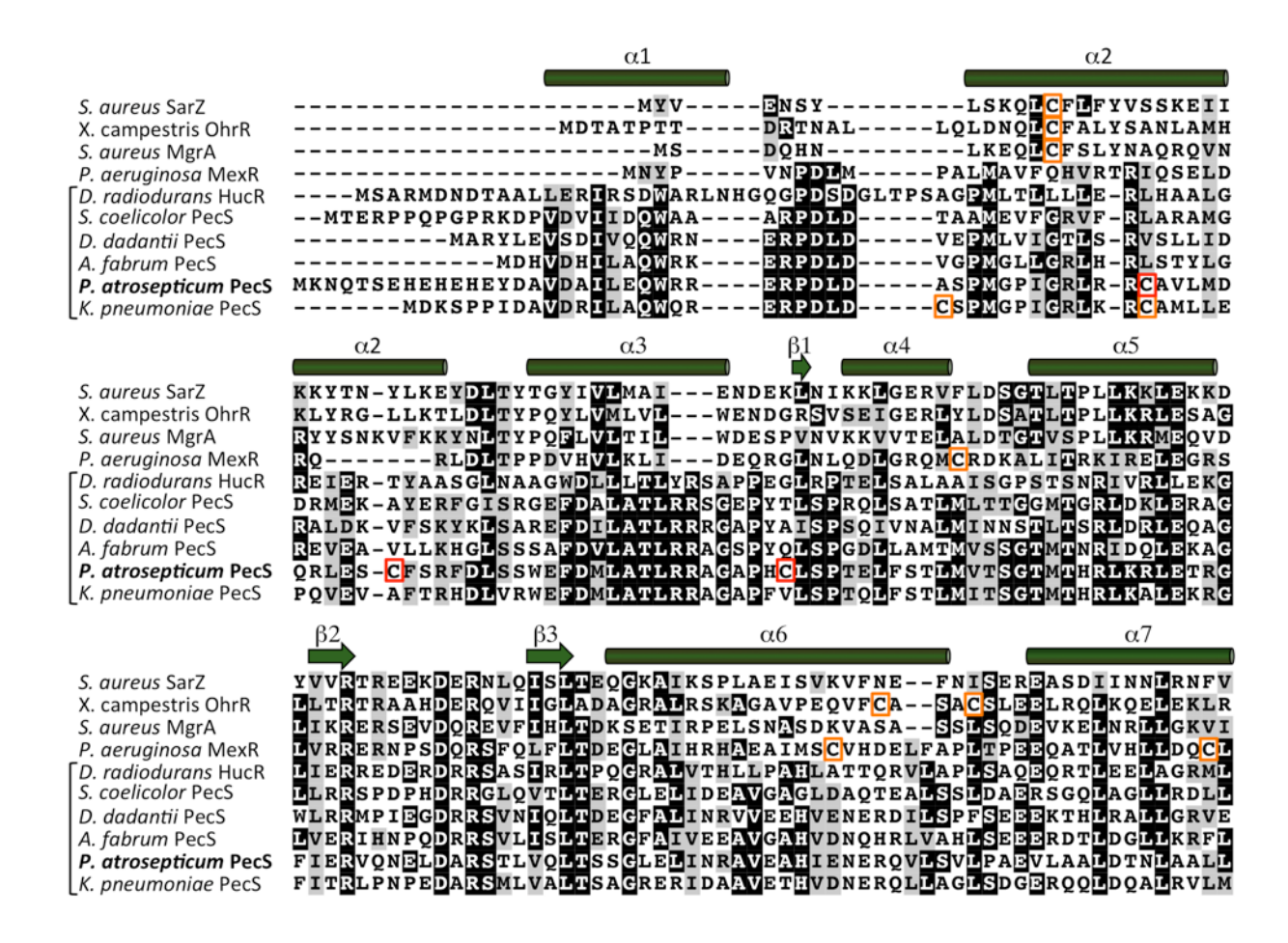


Figure 2. Alignment of MarR homologs. Secondary structure elements are based on the structure of *D. radiodurans* HucR.²⁴ Representative PecS protein sequences are shown, along with sequences of select oxidant-sensing MarR proteins. HucR and PecS belong to the urate-responsive MarR subfamily (bracket).²¹ Cysteine residues in *P. atrosepticum* PecS identified by red boxes, those in other MarR proteins by orange boxes. Sequences are truncated by a few amino acids at their C-termini.

between helices $\alpha 3$ and $\alpha 4$ that are part of the DNA-binding lobe (Fig. 1BC). The comparison of sequence and model of *P. atrosepticum* PecS with well-characterized peroxide-sensing regulators such as OhrR, MexR, and MgrA shows that the cysteine residues of PecS are in

different positions; notably, C45 is conserved in *K. pneumoniae* PecS (Fig. 2). The shortest distance between pairs of cysteine residues is between C45 and C45' from each monomer (~12 Å), suggesting that any disulfide bond formation would require marked conformational changes. By comparison, *Xanthomonas campestris* OhrR forms an inter-subunit disulfide bond between C22 and C127' upon oxidation; these cysteines are separated by 15.5 Å in reduced OhrR.²⁵

Effect of oxidation on conformation of PecS

Reduced PecS exists as a non-covalently linked dimer in solution, as determined by size exclusion chromatography.¹² To investigate the effect of oxidants on oligomeric state of PecS, purified PecS (15 μM) was treated with different concentrations of inorganic (H₂O₂) and organic oxidizing agents (cumene hydroperoxide (CHP) and *tert*-butyl hydroperoxide (TBP)) and separated using non-reducing SDS-PAGE. The oxidation of PecS resulted in formation of intermolecular disulfide bonds, as evidenced by the appearance of dimeric and oligomeric species; PecS was oxidized at similar concentrations by both organic and inorganic oxidants, and the addition of β-mercaptoethanol to oxidized protein lead to conversion of all dimeric and multimeric species to monomeric form, indicating reversible disulfide linkages (Fig. 3AB).

To identify possible disulfide-bonding residues, we created two mutants, PecS-C45A and PecS-C81A. C45 is located at the dimer interface (helix α 2) and C81 in the loop between helix α 3 and α 4 (Fig. 1B); C45 was targeted for mutagenesis as the predicted ~12 Å distance between C45/C45' suggested it as the most likely residue to participate in inter-monomer disulfide bonding (and it is conserved in *K. pneumoniae* PecS), and C81 was targeted due to its predicted surface exposure within the DNA-binding lobe and most likely participation in inter-dimer disulfide bond formation. As shown in Fig. 3C, oxidation of PecS-C45A also gave rise to both

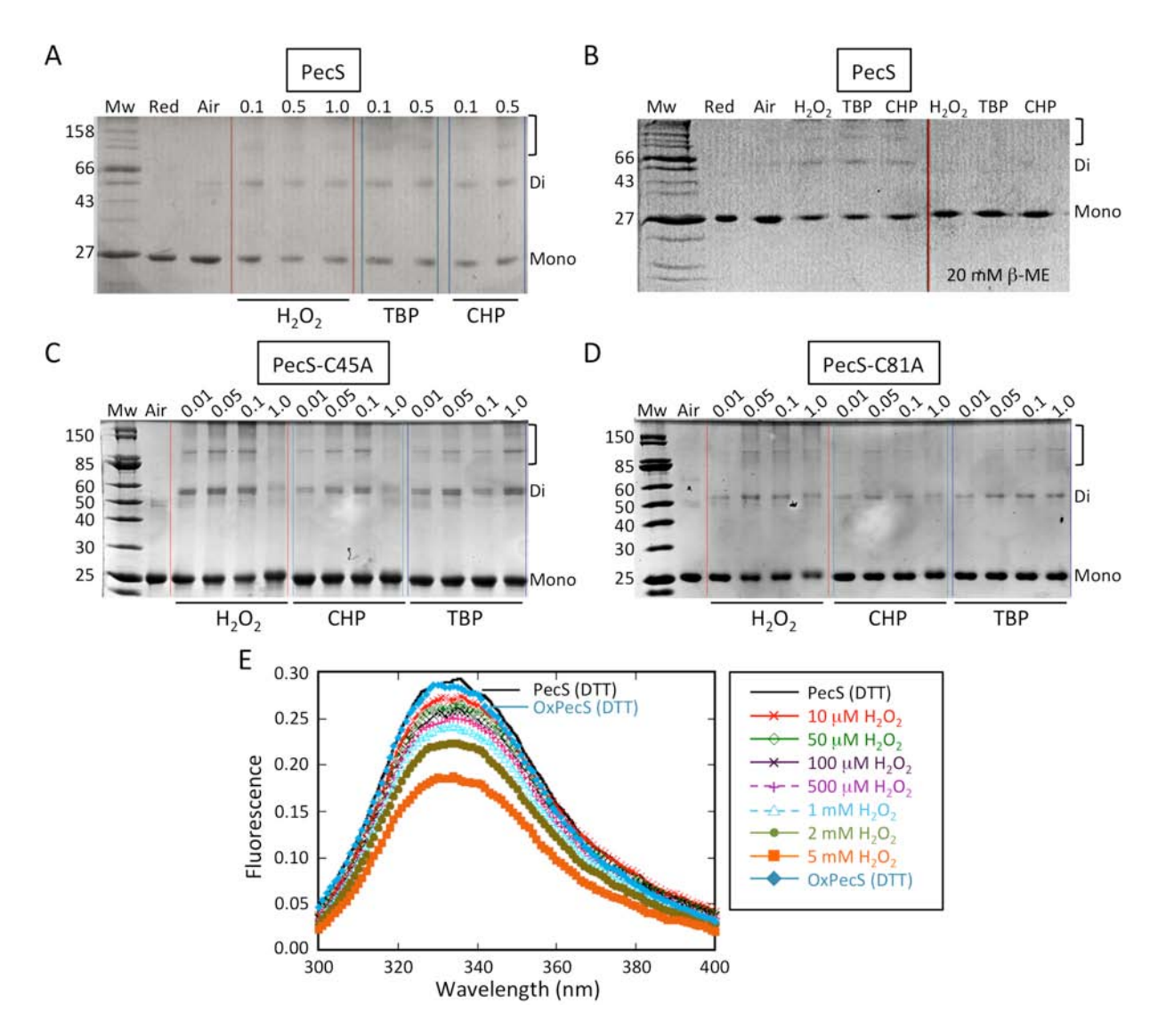


Figure 3. Oxidation of PecS. A. Reduced and oxidized PecS resolved on 15% non-reducing SDS-PAGE gels. Oxidants are identified at the bottom, with concentrations (in mM) at the top. Red, reduced; Air, exposed to air. Monomer (Mono), dimer (Di), and oligomer (bracket) identified at the right. The migration of PecS reflects its calculated Mw of ~20 kDa plus ~3 kDa the N-terminal His₆-tag. B. Reversibility of multimer formation by addition of β-mercaptoethanol. Oxidants are identified at the top (0.5 mM). C-D. Oxidation of PecS-C45A (C) and PecS-C81A (D). Oxidants are identified below the gels, with concentrations (in mM) at the top. E. Fluorescence spectrum of reduced PecS (black line) and PecS incubated with increasing

concentrations of H₂O₂. Oxidized PecS subsequently re-reduced with DTT is shown in turquoise (filled diamond).

dimeric and multimeric species. Since C81/C81' are on opposite faces of the dimer and the predicted distance between C56 and C56' is ~35 Å, we surmise that the dimeric species is a *trans*-dimer between C56 and/or C81 in two monomers in separate PecS dimers. PecS-C81A also yielded both dimeric and multimeric species on oxidation (Fig. 3D); while dimeric species may be due to disulfide-bonding of C56/C56' in *trans*-dimers or to disulfide-linked C45/C45' in a *cis*-dimer, the presence of oligomeric species implies the formation of C45/C45' disulfide bonds. In all cases, most of the protein remained monomeric.

To examine the impact of oxidation on the conformation of wild-type PecS, we measured intrinsic tryptophan fluorescence. *P. atrosepticum* PecS contains two tryptophans, W24 in α 1 (within the urate-binding pocket) and W65 at the N-terminus of α 3, and the fluorescence spectrum reveals peak fluorescence around 336 nm (Fig. 3; black line). The oxidation of PecS with increasing concentration of H_2O_2 (10 μ M to 5 mM) resulted in gradual quenching of intrinsic fluorescence intensity, which shows that oxidation imposes a change in the local environment of one or both tryptophan residues. Notably, the observed decrease in fluorescence intensity was fully reversible upon treating the oxidized protein with DTT (Fig. 3; turquoise filled diamonds)). The complete reversibility also indicates that reduced fluorescence was not due to loss of protein as a result of precipitation.

To assess the effect of oxidation on PecS stability, we determined thermal stability of reduced and oxidized protein by differential scanning fluorometry. The intensity of fluorescence emission induced by binding of SYPRO orange dye to hydrophobic regions of unfolded protein was

measured as a function of temperature (Fig. 4AB). The oxidation of PecS with lower concentration (10 μ M and 100 μ M) of H₂O₂ or CHP resulted in a modest decrease in the melting temperature of PecS (Tm = 50.0 \pm 0.4 °C) by ~2-4 °C, with the greatest decrease in Tm seen on oxidation with CHP, whereas exposure of PecS to higher oxidant concentration (1 mM or 2 mM) led to further decrease in melting temperature by ~8-10 °C (Table 1). Taken together, these data suggest that oxidation induces a change in the conformation of PecS by both inorganic and organic oxidants, with the organic oxidant CHP impacting the stability of PecS somewhat more efficiently at lower concentrations.

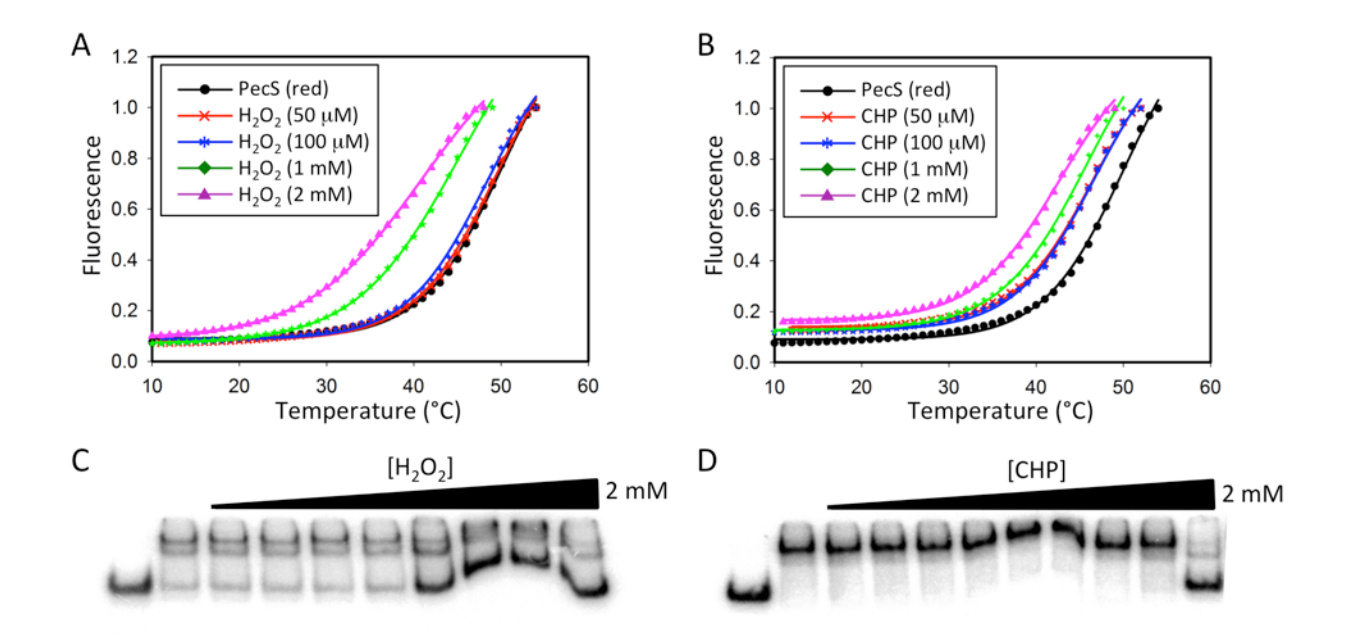


Figure 4. PecS oxidation reduces thermal stability, but not DNA complex formation. A-B. Thermal denaturation represented by fluorescence of SYPRO Orange dye bound to hydrophobic regions of unfolded protein as a function of temperature. C-D. Electrophoretic mobility shift assay of PecS bound to *pecS-pecM* intergenic DNA as a function of H₂O₂ (C) or CHP (D) concentration.

Table 1. Thermal stability of reduced and oxidized PecS

Tm (°C)
48.2 ± 0.3
47.9 ± 0.3
46.9 ± 0.3
42.7 ± 0.4
39.2 ± 0.3
45.1 ± 0.3
45.2 ± 0.3
43.7 ± 0.4
41.4 ± 0.3

Oxidation of PecS attenuates DNA distortion

The effect of oxidation on DNA binding by PecS was determined by electrophoretic mobility shift assays (EMSA) performed under reducing and oxidizing conditions. Previously, we have

shown that reduced PecS binds pecO (92 bp), consisting of the pecS-pecM intergenic region with high affinity ($K_d = 1.0 \pm 0.1$ nM) and specificity at neutral pH.¹² While conformational changes in oxidized PecS were inferred based on changes in Trp fluorescence and thermal stability, oxidation of PecS with H_2O_2 or CHP (10 μ M - 2 mM) did not affect complex formation by PecS appreciably, except at very high concentration of oxidizing agents where binding was compromised (Fig. 4CD).

To examine the DNA binding by oxidized PecS more carefully, we used DNase I footprinting and determined digestion patterns using fragment analysis.²⁰ A 317 bp fluorescently labeled DNA containing the *pecS-pecM* intergenic region was incubated with or without PecS before DNase I digestion. As reported previously, reduced PecS (28 nM, representing a PecS:DNA ratio of 2:1) protected two areas, S1 and S2, spanning from -18 to +4 (23 bp) and from -57 to -34 (24 bp), relative to the start codon of the PecS open reading frame (and with S2 encompassing sequence 5 bp upstream of the start codon for PecM; Fig. 5A,E). Marked hypersensitive cleavage sites flanking each protected region were observed at positions -64, -33, -32, -26, -25, and +6, implying that reduced PecS induces significant DNA distortion upon binding. To note, both protected areas correspond to the predicted palindromes and are identical to the previously reported sites, including hypersensitive cleavage sites.¹²

The footprint of oxidized PecS showed an identical protection pattern compared to reduced protein, indicating that specificity was not compromised on oxidation (Fig. 5B). However, hypersensitive cleavage sites were absent, even though complete protection of both palindromes was observed at the same concentration (28 nM) required for complete protection by reduced PecS. A key conclusion from these observations is that only reduced PecS induced marked DNA distortion upon binding.

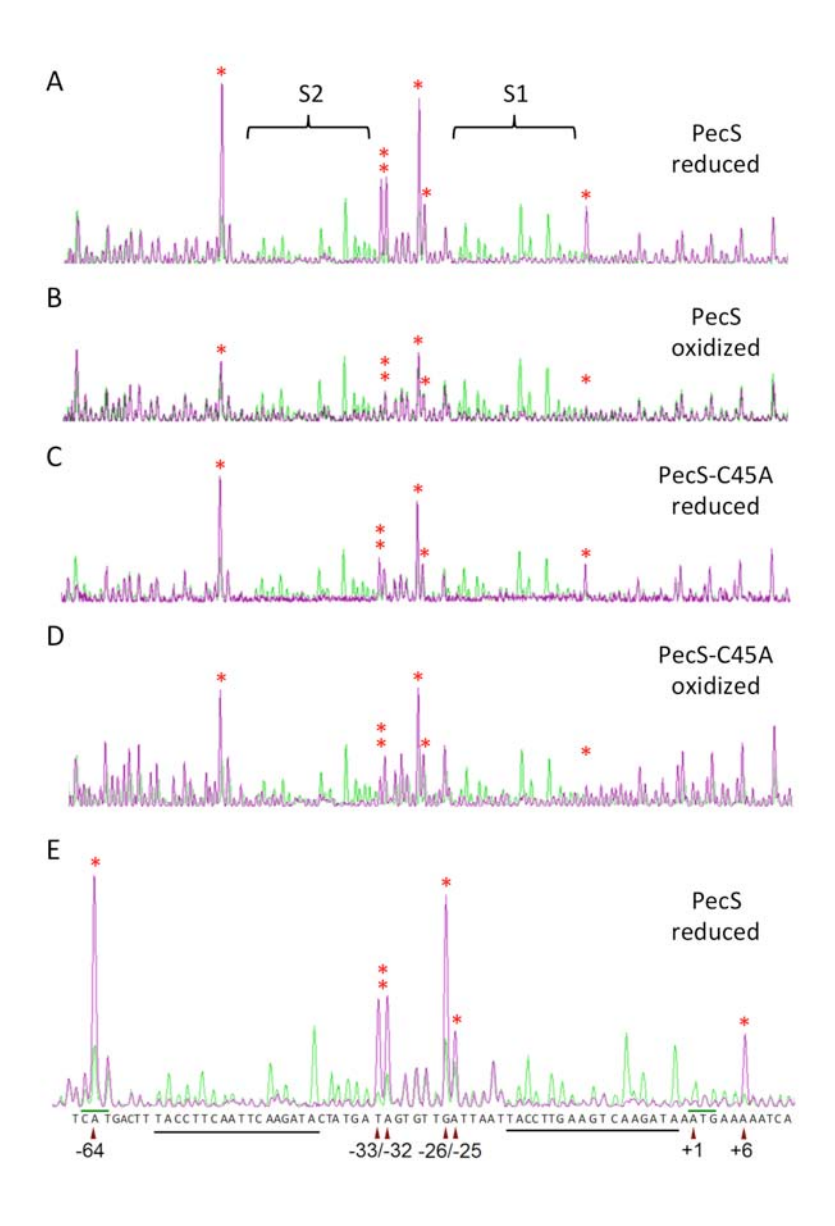


Figure 5. DNase I footprints of reduced and oxidized PecS. A. DNase I digestion of *pecS-pecM* intergenic DNA without (green) or with reduced WT PecS (28 nM, representing a stoichiometric ratio of PecS:DNA of 2:1; magenta). Two protected regions (S1 and S2) identified by brackets. B. DNase I digestion of DNA without (green) or with oxidized WT PecS (28 nM; magenta). C. DNase I digestion of DNA without (green) or with reduced PecS-C45A (28 nM; magenta). D. DNase I digestion of DNA without (green) or with oxidized PecS-C45A (28 nM; magenta). The y-axis (in arbitrary units) is constant in panels A-D, as reflected in comparable heights of peaks

at the far left and far right, where cleavage was unaffected by protein addition. E. Expanded view of protected pseudopalindromic sites S1 and S2 from panel A; sequence is shown, and palindromes are underlined. Translational start sites for PecM (-63) and PecS (defined as +1) marked with green lines above the sequence. Hypersensitive cleavage imposed by PecS binding is identified by asterisks. Experiments were performed under stoichiometric conditions ([DNA]>>Kd). Representative of at least three independent experiments.

Footprinting performed with both reduced and oxidized PecS-C45A (28 nM) showed a similar protection pattern as for wild-type PecS (Fig. 5CD). The complete protection suggests that the reaction was performed under stoichiometric conditions ([DNA]>>Kd) as for wild-type PecS. Notably, the flanking hypersensitive sites were present at identical positions as for WT PecS, except that hypersensitive cleavage was less pronounced, and complete protection was observed at the same protein concentration. These data suggest that DNA binding by reduced PecS-C45A was insensitive to oxidation. Accordingly, we infer that oxidation of C45 is required for changes in the DNA-binding mode of wild-type PecS (loss of DNA distortion) to be manifest.

In contrast, footprinting carried out with reduced and oxidized PecS-C81A (28 nM) did not show any protection, suggesting reduced affinity and/or loss of specificity (data not shown). At higher concentration (140 nM), reduced PecS-C81A did protect a site corresponding to that of wild type PecS, indicating that specificity was retained (Fig. 6A). Since no protection was detectable using 28 nM PecS-C81A, but complete protection was seen at 140 nM protein, we infer that the apparent binding constant of PecS-C81A for this DNA must be >28 nM (as a Kd of 28 nM or lower would result in at least 50% protection using 28 nM protein), but lower than 140

nM. However, ultra-hypersensitive cleavage sites were observed at the positions where wild-type PecS induced hypersensitive cleavage, suggesting very pronounced DNA distortions imposed by binding of PecS-C81A. In contrast, at the same concentration, oxidized PecS-C81A did not induce any DNA distortion as evidenced by absence of hypersensitive cleavage. Quantitation of hypersensitive cleavage confirms the key inferences made by visual inspection, namely that oxidation of both wild-type PecS and PecS-C81A results in loss of hypersensitive cleavage, and that hypersensitive cleavage observed with PecS-C45A is reduced relative to wild-type PecS and insensitive to oxidation (Fig. 7AB). These observations are consistent with the interpretation that it is oxidation of C45 that induces a protein conformation that does not lead to DNA distortion.

The conservation of palindromic sequences suggests PecS recognition by direct readout, likely accomplished by major groove binding of recognition helices. However, analysis of the *pecS-pecM* intergenic region and flanking coding sequences using DNAshape predicts that PecS binding sites are characterized by very narrow minor grooves (by comparison to the 5.8 Å width in ideal *B*-form DNA) and therefore a widening of the opposing major grooves, a feature that is not seen in the surrounding sequence (Fig. 7C). Such intrinsically narrow DNA minor grooves locally enhance negative electrostatic potential and have been associated with the binding of positively charged (mainly Arg) residues.²⁶ Indeed, the "wing" component of the wHTH motif (β 2- β 3; Fig. 2) would be expected to contact the minor groove.⁵ The exact mode of binding notwithstanding, the analysis suggests that PecS also uses DNA shape recognition for identification of cognate sites.

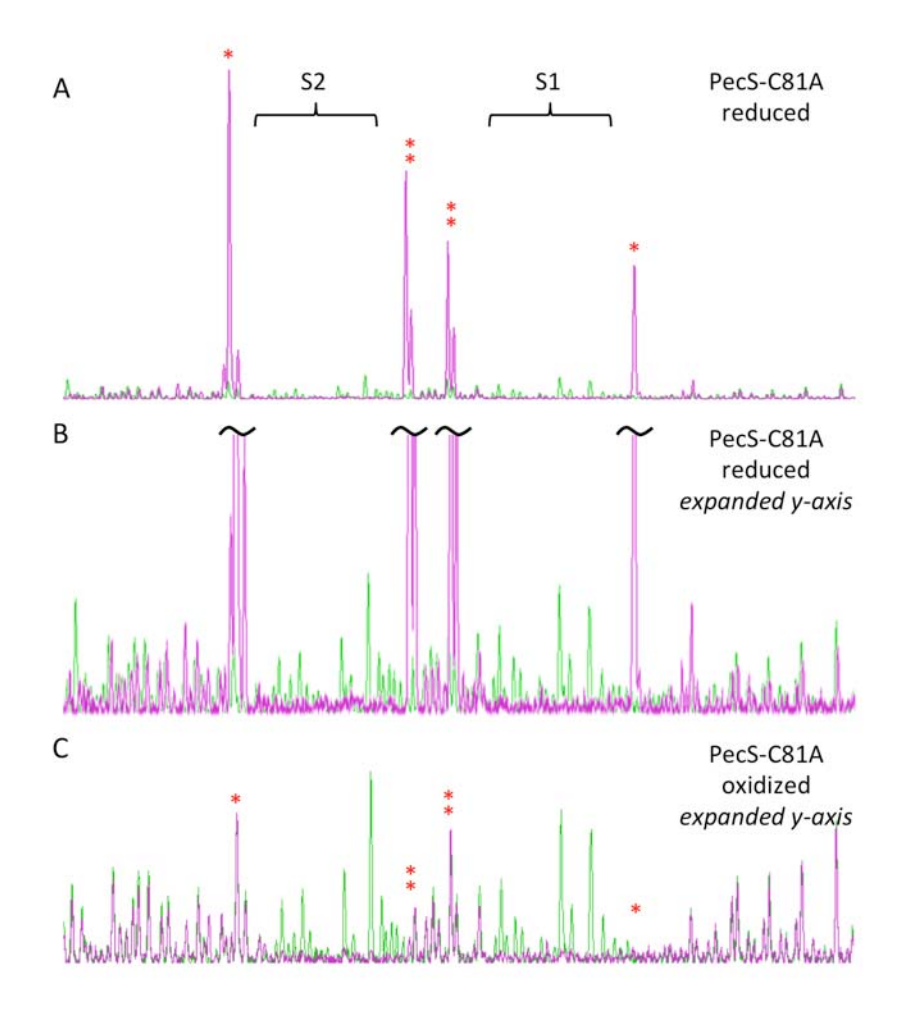


Figure 6. DNase I footprint of PecS-C81A. A. DNase I digestion of DNA without (green) or with reduced PecS-C81A (140 nM; magenta); lower panel shows the same region, except with an expanded y-axis and hypersensitive sites truncated to illustrate protected region. B. DNase I digestion of DNA without (green) or with oxidized PecS-C81A (140 nM; magenta). Asterisks indicate the positions of hypersensitive cleavage seen with reduced protein. Representative of at least three independent experiments.

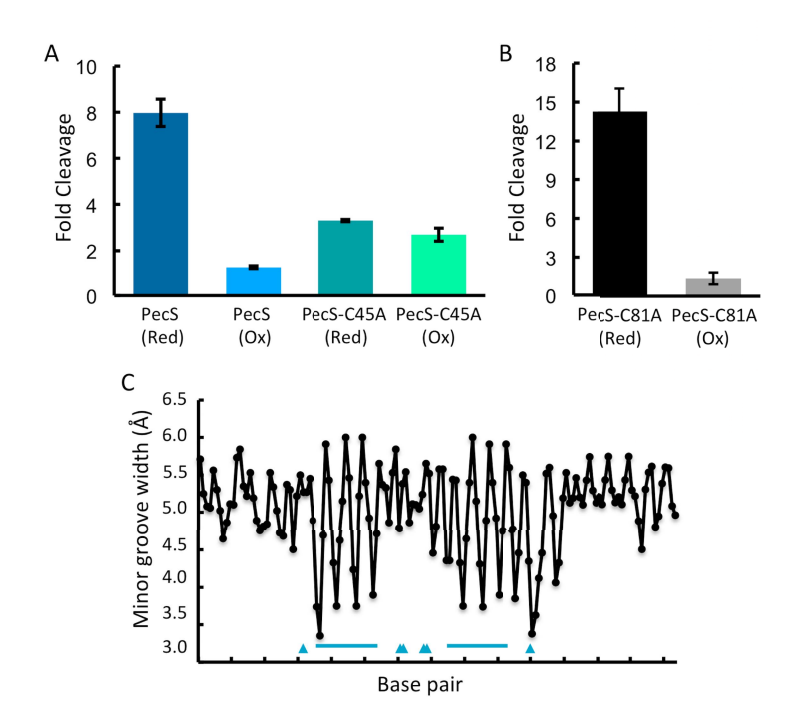


Figure 7. Features of PecS binding sites. A-B. Quantitation of hypersensitive cleavage sites. The relative intensity of hypersensitive sites identified in Figs. 5 and 6 was totaled and normalized to the intensity of the same sites in DNA to which no PecS was added. Error bars represent standard deviation. C. Predicted values of minor groove width as a function of base pair (tick marks every 10 bp). The *pecS-pecM* intergenic sequence and flanking coding sequences were analyzed by DNAshape, which predicts intrinsic DNA structural features using a Monte Carlo approach.²⁷ Horizontal lines represent the palindromic sequences identified in Fig. 5E, and arrowheads identify hypersensitive cleavage sites.

PecS-mediated response to oxidants in vivo

PecS-mediated repression of *pecS* promoter activity was assessed using a transcriptional reporter in which enhanced green fluorescent protein (EGFP) was expressed under control of the *pecS* promoter (*pecO*). ¹² E. *coli* cells harboring this construct (pACYC184_EGFP-pecO) as well

as pET100-pecS in which *pecS* expression was not induced by addition of IPTG showed ample EGFP expression (Fig. 8B). Induction of *pecS* expression by IPTG resulted in reduced production of EGFP and no green fluorescence was observed (Fig. 8C). Notably, addition of H₂O₂ to IPTG-induced cultures restored green fluorescence (Fig. 8D). These data indicate that the repression of the *pecS* promoter that is imposed by PecS under reducing conditions is relieved on addition of oxidant. By contrast, IPTG induction of neither *pecS-C45A* nor *pecS-C81A* led to repression of EGFP production (Fig. 9B,D). This is consistent with attenuated DNA distortion imposed by PecS-C45A, as evidenced by reduced hypersensitive cleavage (Figs. 5C and 7A), and with the inference that the affinity of PecS-C81A for cognate DNA is reduced compared to wild-type PecS.

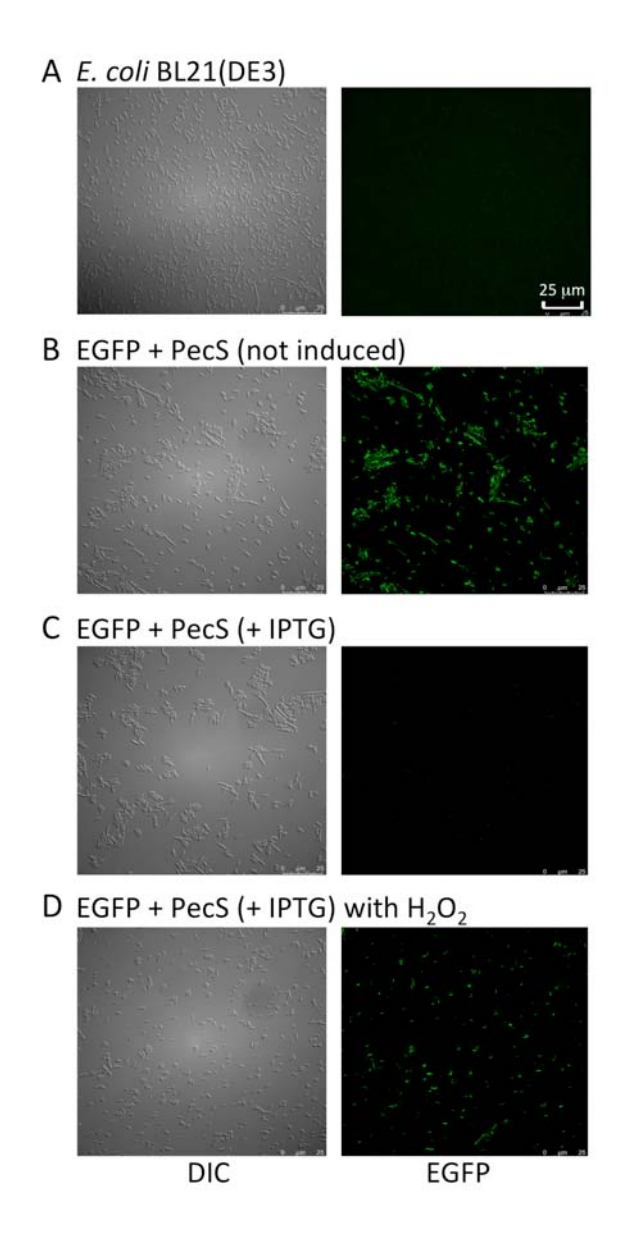


Figure 8. Only reduced PecS represses the *pecS* promoter *in vivo*. Phase contrast (left) and fluorescent micrographs (right) are shown. A. E. coli BL21 harboring no plasmids. B-D. E. coli BL21 transformed with pACYC184_EGFP-pecO and pET100-pecS. B No IPTG induction. C. With IPTG induction of *pecS*. D. With addition of H₂O₂ along with IPTG induction. DIC, differential interference contrast. The scale bar in (A) represents 25 μm and is the same for all micrographs. Representative of at least three independent experiments.

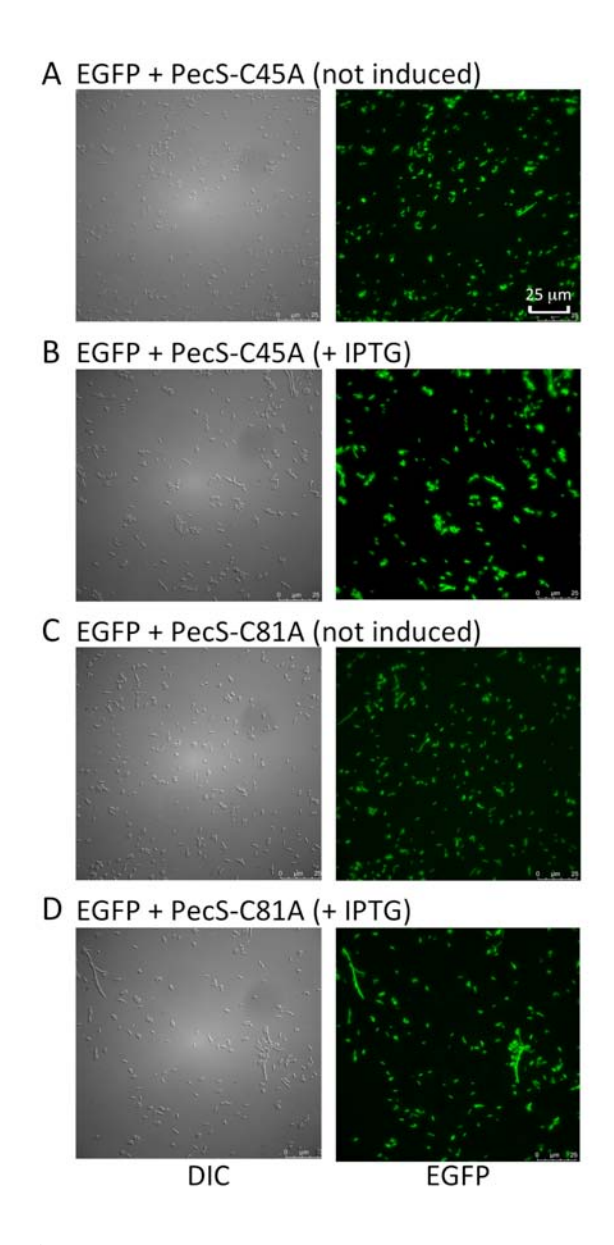


Figure 9. Neither PecS-C45A, nor PecS-C81A repress the *pecS* promoter *in vivo*. Phase contrast (left) and fluorescent micrographs (right) are shown. A-B. *E. coli* BL21 harboring pACYC184_EGFP-pecO and pET100-pecS-C45A without (A) or with IPTG-induction (B). C-D. *E. coli* BL21 harboring pACYC184_EGFP-pecO and pET100-pecS-C81A without (C) or with IPTG-induction (D). DIC, differential interference contrast. The scale bar in (A) represents 25 μm and is the same for all micrographs. Representative of at least three independent experiments.

Oxidation-responsive transcriptional regulation by PecS

To examine further how PecS oxidation impacts its function as a transcriptional repressor, a DNA construct was created in which divergent run-off transcripts of 144 and 67 nt would be generated by E. coli RNA polymerase, with each transcript produced under control of the pecS and pecM promoters, respectively. An in vitro transcription assay was performed in which reduced or oxidized PecS was incubated with the DNA template, transcription was initiated by addition of NTPs and E. coli RNA polymerase holoenzyme, and transcripts were identified by denaturing polyacrylamide gel electrophoresis (Fig. 10). In the control experiment, which was performed without addition of PecS, the two transcripts of expected length (144 and 67 bp) were generated. Notably, the intensity of both transcripts was gradually reduced on addition of increasing concentrations of reduced PecS, suggesting that transcription was repressed by PecS (Fig. 10A,C). Consistent with the presence of two binding sites in the pecS-pecM DNA, repression was most efficient at a ratio of dimeric PecS:DNA of 2:1. In contrast, the oxidized protein failed to repress transcription, as two transcripts were generated at an abundance comparable to the control (Fig. 10B,C). Similarly, neither PecS-C45A, nor PecS-C81A were able to repress transcription in vitro regardless of whether the proteins were reduced or oxidized (Fig. 11). These data are consistent with the interpretation that DNA distortion imposed by PecS is required for efficient repression of the pecS and pecM promoters, and the observed repression is consistent with that observed in vivo.

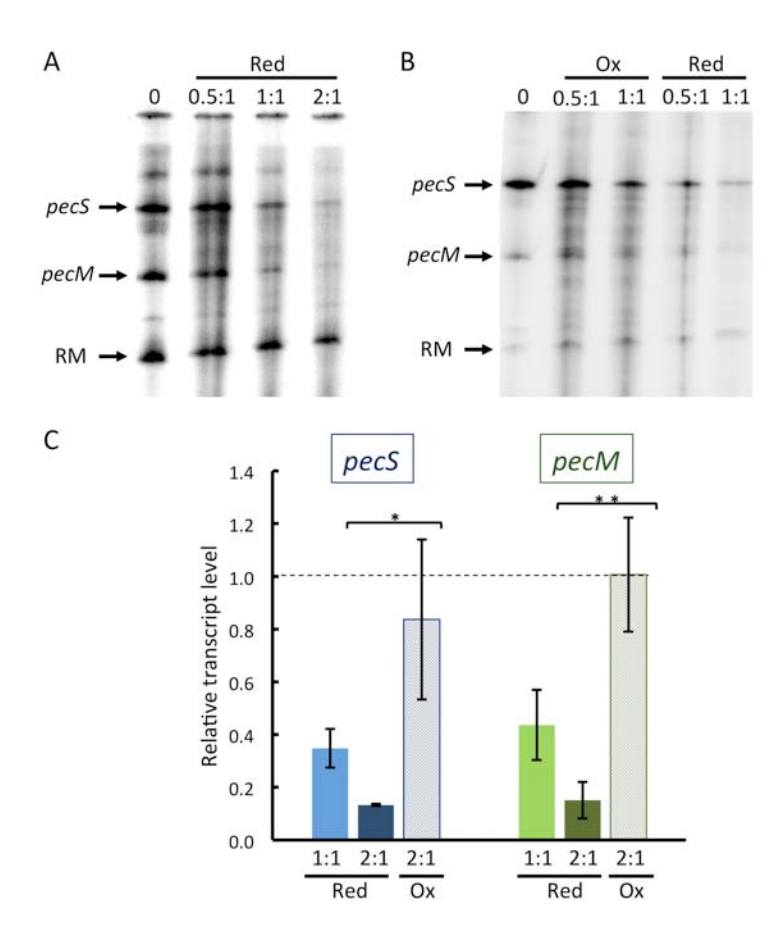


Figure 10. Only reduced PecS represses transcription *in vitro*. A-B. Denaturing gels showing transcripts formed *in vitro* using a DNA template from which two run-off transcripts are produced. Transcripts are produced under control of either *pecS* or *pecM* promoters, as identified at the left. RM is recovery marker. Molar ratios of dimeric PecS:DNA are identified at the top; Red, reduced protein; Ox, oxidized protein; 0, no PecS. C. Relative transcript levels at the indicated ratios of reduced (Red) or oxidized (Ox) PecS:DNA; transcript levels are reported relative to reactions without PecS (dotted line). Transcript levels from individual reactions are calculated relative to the recovery marker. This procedure corrects for any differences in loading. Reactions were performed in triplicate. Asterisks indicate statistically significant difference based on a Student's t-test; *, p< 0.05; **, p<0.01).

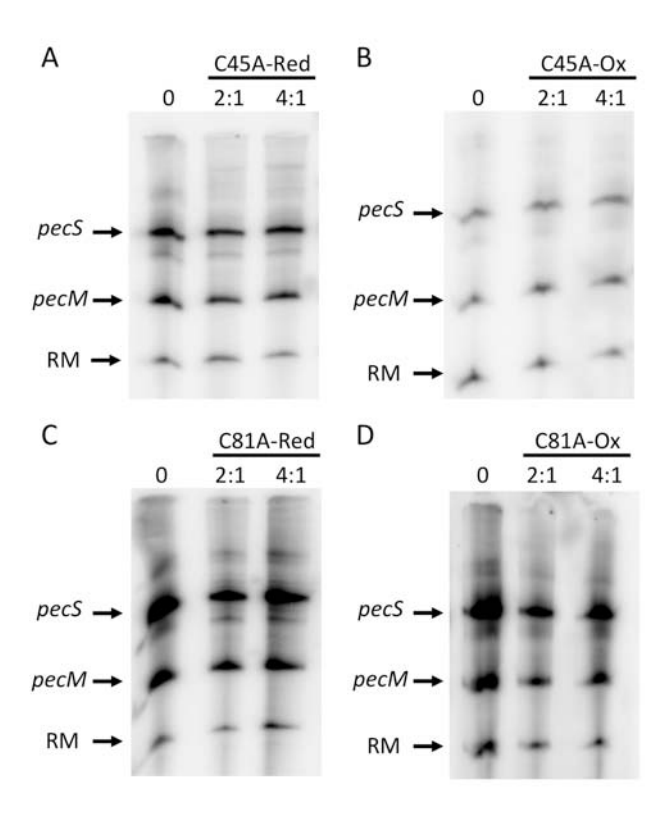


Figure 11. Neither PecS-C45A, nor PecS-C81A repress transcription *in vitro*. Denaturing gels showing transcripts produced under control of either *pecS* or *pecM* promoters, as identified at the left. RM is recovery marker. Molar ratios of dimeric PecS:DNA are identified at the top; Red, reduced protein; Ox, oxidized protein; 0, no PecS.

Discussion

Distinct conformations of promoter DNA in complex with reduced or oxidized PecS

Hypersensitive DNA cleavage by DNaseI indicates enhanced accessibility of the enzyme to specific sites, an accessibility that is attributable to PecS-mediated DNA distortions. Since the hypersensitive cleavage, and by extension the DNA distortion, is attenuated on oxidation of wild-type PecS and PecS-C81A, but not on oxidation of PecS-C45A (Figs. 5 and 6), we infer that it is oxidation of C45 that leads to the altered binding mode. C45 is near the pivot point of

the long α2 helices that form the scaffold for the dimer interface (Fig. 1B). A disulfide bond between C45 and C45' from the other monomer could account for the reversible dimeric species observed on oxidation (Fig. 3AB), and the ~12 Å distance between these residues suggests that disulfide bond formation would require substantial conformational changes; such conformational changes could result in the reduced thermal stability and tryptophan fluorescence that is associated with PecS oxidation (Figs. 3C and 4AB). As noted above, very marked conformational changes occur on disulfide bond formation in X. xampestris OhrR. 25 However, in Bacillus subtilis OhrR, the initial oxidation of a target cysteine to form an unstable sulfenic acid may be followed by further oxidation to sulfonic or sulfinic acid in absence of disulfide-bonding partner.²⁸ The precise oxidation products notwithstanding, our data indicate that C45 oxidation leads to an altered DNA binding mode that is not associated with transcriptional repression. The very marked hypersensitive cleavage seen in DNA bound by reduced PecS-C81A implies an even more extensive DNA distortion compared to that imposed by wild-type PecS; C81 is in the loop between $\alpha 3$ and $\alpha 4$, and its substitution may result in a disposition of recognition helices that requires further DNA distortion for binding. Accordingly, the reduced affinity of PecS-C81A may be a result of DNA binding energy being expended on this additional DNA distortion. That changes to the dimer interface can result in attenuated DNA binding has been previously

reported for other MarR proteins. For example, the location of C45 near the crossover point of scaffold helices is reminiscent of the position of a pH-sensing histidine in HucR from *Deinococcus radiodurans*. In the case of HucR, a decrease in pH causes protonation of this histidine, a consequence of which is charge repulsion between the histidines from each monomer and that DNA binding is reduced.²³ Similarly, substitution of a glutamine in *Staphylococcus aureus* MepR that is also located in the middle of the scaffold helices (α1 in this case) markedly

reduces DNA binding affinity as it precludes optimal orientation of recognition helices.²⁹ In case of MepR, this mutation is among several that are associated with multidrug resistance, as MepR controls expression of gene encoding the efflux pump MepA. Taken together, we suggest that oxidation of C45/C45' in *P. atrosepticum* PecS causes structural changes in the dimerization region that are transmitted to the DNA-binding lobes.

Oxidized PecS protects two sites in the *pecS-pecM* intergenic region, but binding is not associated with hypersensitive cleavage (Fig. 5B). By contrast, DNA binding by reduced PecS requires a conformational change in the DNA that leads to enhanced DNaseI cleavage (Fig. 5A). Since mobility of PecS-DNA complexes is unaffected by amino acid substitutions or addition of oxidant (Fig. 4CD and data not shown), and since substantial DNA bending should be associated with detectable retardation of the resulting complex in DNA of the length used here, we surmise that PecS does not induce a net DNA bend. The 38 bp distance between the centers of palindromes (Fig. 5E) suggests that two PecS dimers bind on opposite faces of the DNA duplex, assuming *B*-form DNA. Such asymmetry of binding, which is also reflected in the footprint (each protected region being flanked by either one or two hypersensitive sites) could produce two bends that are out of phase with the helical repeat, resulting in no net bend. An alternate explanation is that PecS primarily imposes a change in twist.

The ability of transcriptional regulators to induce differential changes in promoter architecture that correlate with gene activity has been previously reported. For example, structural studies of the $E.\ coli$ copper efflux regulator CueR, a member of the MerR protein family, reveal that changes in DNA conformation due to protein binding result in realigning of core promoter elements for differential gene expression. The repressor conformation of CueR under-twists the DNA to shorten the promoter element by ~ 3 Å to prevent gene transcription, and the DNA

under-twisting and bending is reflected in DNase I hypersensitive sites in the CueR/DNA complex. These changes to promoter DNA topology were proposed to impose an energetic barrier to transcription.^{31,32} We speculate that PecS may likewise impose conformational changes in promoter DNA that adversely affect the ability of RNA polymerase to bind or initiate transcription, but only under reducing conditions. When PecS is oxidized, DNA binding is no longer associated with significant changes in DNA conformation, allowing RNA polymerase to displace PecS (Fig. 12).

The possibility that PecS uses shape recognition (indirect readout; Fig. 7C) for identification of cognate sites is intriguing for a variety of reasons. It may relax the specific sequence requirement and allow interaction with more degenerate sequences, a feature characteristic of *D. dadantii* PecS.³³ Such plasticity may facilitate the development of novel regulatory circuits. It also suggests that environmental factors, including acid and oxidative stress, which influence DNA topology, have the potential to alter DNA binding and in turn gene regulation by PecS.^{34, 35} Analysis of the extent to which PecS can repress transcription from the *pecS/pecM* promoters in covalently closed circular DNA of varying superhelical density could prove instructive in this context.

Physiological relevance

The success of plant pathogens relies on their ability to adapt to the hostile environment that characterizes the host tissue. The plant responds to invading bacteria by production of ROS that are for example generated by plasma membrane-bound NADPH oxidase and by the enzyme xanthine dehydrogenase, which resides in the peroxisomal matrix (Fig. 12). Xanthine oxidase, which is also found in the cytoplasm, converts hypoxanthine to xanthine and xanthine to urate

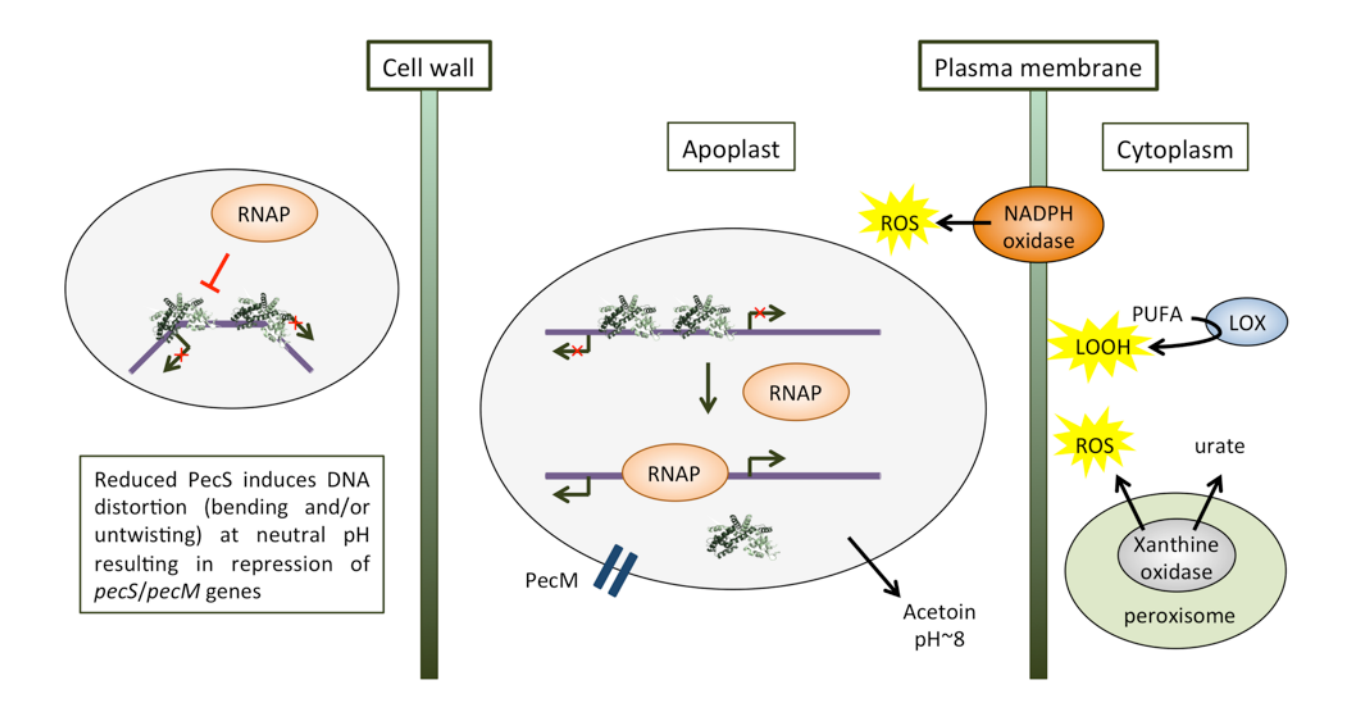


Figure 12. Conformations of PecS-bound promoter DNA control gene expression. Reduced PecS (green) induces DNA distortion at neutral pH, resulting in repression of *pecS/pecM* genes prior to infection of a plant host (left). Upon colonization of the plant apoplast (center), bacteria produce acetoin to raise the pH and they encounter ROS produced by the host. Under these conditions, oxidized PecS binds DNA to generate a conformation compatible with RNA polymerase binding, allowing transcription and production of PecS and PecM. Examples of ROS sources are plasma membrane-bound NADPH oxidase (orange oval) and xanthine oxidase (gray), which resides in the peroxisomal matrix (right). Lipoxygenase (LOX) enzymes generate lipid hydroperoxides (LOOH) from polyunsaturated fatty acids (PUFA).

along with ROS production, and both xanthine and urate accumulate when the enzyme is active. ¹⁴ In addition, lipid hydroperoxides derived from polyunsaturated fatty acids (PUFA) have been reported to contribute to anti-microbial defenses. ³⁶ The comparable concentrations at with both inorganic (H₂O₂) and organic (CHP) oxidants oxidize PecS *in vitro* (Figs. 3 and 4) raises the possibility that PecS responds to different types of oxidants in the plant apoplast. The structure model of PecS suggests that Cys45 is predicted to face a very hydrophobic pocket that is lined by mostly leucine residues (Fig. 1C). These structural features would be consistent with oxidation of Cys45 by organic hydroperoxides such as the lipid hydroperoxides (oxylipins) that are formed in the course of the host defense, ³⁶ an inference that is supported by the efficient oxidation of PecS by organic oxidants *in vitro* (Figs. 3 and 4).

For phytopathogens such as *P. atrosepticum*, the onset of virulence gene expression begins with alkalinization of the plant apoplast, which is required for optimal function of pectinase enzymes. Another urgent matter is to mount a defense against host-generated ROS. Our data suggest that *P. atrosepticum* PecS responds to several cues that characterize the host environment. Notably, both an increase in pH and protein oxidation is associated with a change in DNA binding that enables RNA polymerase to displace PecS while urate-binding results in attenuated DNA binding. By responding to several distinct signals that originate in different cellular locations, the outcome may be more efficient induction of the PecS regulon. While the *D. dadantii* PecS regulon has been characterized and shown to include numerous virulence genes, PecS orthologs from different species are likely to control a distinct set of genes, reflecting a rapid evolution of gene regulatory networks. It would therefore be of interest to compare the PecS regulons from the related phytopathogens *D. dadantii* and *P. atrosepticum*.

Acknowledgments. We thank D. Burk from the LSU Socolofsky Microscopy Center for

assistance with fluorescence microscopy. Support from the National Science Foundation (MCB-

1714219 to A.G.) and by an award to LSU under the HHMI Science Education Program is

gratefully acknowledged.

Abbreviations used: EMSA, electrophoretic mobility shift assay; IPTG, isopropyl β-D-1-

thiogalactopyranoside; MarR, multiple antibiotic resistance regulator; ROS, reactive oxygen

species

Accession ID: P. atrosepticum PecS - Q6D5K4

36

References

- [1] Knoefler, D., Leichert, L. I., Thamsen, M., Cremers, C. M., Reichmann, D., Gray, M. J., Wholey, W. Y., and Jakob, U. (2014) About the dangers, costs and benefits of living an aerobic lifestyle, *Biochem Soc Trans* 42, 917-921.
- [2] Segal, B. H., Grimm, M. J., Khan, A. N., Han, W., and Blackwell, T. S. (2012) Regulation of innate immunity by NADPH oxidase, *Free Radic Biol Med* 53, 72-80.
- [3] Fang, F. C. (2011) Antimicrobial actions of reactive oxygen species, *MBio* 2, e00141-00111.
- [4] Hillion, M., and Antelmann, H. (2015) Thiol-based redox switches in prokaryotes, *Biol Chem* 396, 415-444.
- [5] Deochand, D. K., and Grove, A. (2017) MarR family transcription factors: dynamic variations on a common scaffold, *Crit Rev Biochem Mol Biol* 52, 595-613.
- [6] Hommais, F., Oger-Desfeux, C., Van Gijsegem, F., Castang, S., Ligori, S., Expert, D., Nasser, W., and Reverchon, S. (2008) PecS is a global regulator of the symptomatic phase in the phytopathogenic bacterium *Erwinia chrysanthemi* 3937, *J Bacteriol* 190, 7508-7522.
- [7] Pedron, J., Chapelle, E., Alunni, B., and Van Gijsegem, F. (2018) Transcriptome analysis of the *Dickeya dadantii* PecS regulon during the early stages of interaction with *Arabidopsis thaliana*, *Mol Plant Pathol* 19, 647-663.

- [8] Reverchon, S., Nasser, W., and Robert-Baudouy, J. (1994) pecS: a locus controlling pectinase, cellulase and blue pigment production in *Erwinia chrysanthemi*, *Mol Microbiol* 11, 1127-1139.
- [9] Wang, Z. C., Liu, C. J., Huang, Y. J., Wang, Y. S., and Peng, H. L. (2015) PecS regulates the urate-responsive expression of type 1 fimbriae in *Klebsiella pneumoniae* CG43, *Microbiology* 161, 2395-2409.
- [10] Perera, I. C., and Grove, A. (2010) Urate is a ligand for the transcriptional regulator PecS, J Mol Biol 402, 539-551.
- [11] Huang, H., Mackel, B. J., and Grove, A. (2013) *Streptomyces coelicolor* encodes a urateresponsive transcriptional regulator with homology to PecS from plant pathogens, *J Bacteriol* 195, 4954-4965.
- [12] Deochand, D. K., Meariman, J. K., and Grove, A. (2016) pH-Dependent DNA Distortion and Repression of Gene Expression by *Pectobacterium atrosepticum* PecS, *ACS Chem Biol* 11, 2049-2056.
- [13] Bhattacharyya, N., Lemon, T. L., and Grove, A. (2019) A role for *Vibrio vulnificus* PecS during hypoxia, *Sci Rep* 9, 2797.
- [14] Ma, X., Wang, W., Bittner, F., Schmidt, N., Berkey, R., Zhang, L., King, H., Zhang, Y., Feng, J., Wen, Y., Tan, L., Li, Y., Zhang, Q., Deng, Z., Xiong, X., and Xiao, S. (2016) Dual and Opposing Roles of Xanthine Dehydrogenase in Defense-Associated Reactive Oxygen Species Metabolism in Arabidopsis, *Plant Cell* 28, 1108-1126.

- [15] Sivapragasam, S., Deochand, D. K., Meariman, J. K., and Grove, A. (2017) The Stringent Response Induced by Phosphate Limitation Promotes Purine Salvage in *Agrobacterium fabrum*, *Biochemistry* 56, 5831-5843.
- [16] Crane, J. K., Naeher, T. M., Broome, J. E., and Boedeker, E. C. (2013) Role of host xanthine oxidase in infection due to enteropathogenic and Shiga-toxigenic *Escherichia coli*, *Infect Immun* 81, 1129-1139.
- [17] Charkowski, A., Blanco, C., Condemine, G., Expert, D., Franza, T., Hayes, C., Hugouvieux-Cotte-Pattat, N., Lopez Solanilla, E., Low, D., Moleleki, L., Pirhonen, M., Pitman, A., Perna, N., Reverchon, S., Rodriguez Palenzuela, P., San Francisco, M., Toth, I., Tsuyumu, S., van der Waals, J., van der Wolf, J., Van Gijsegem, F., Yang, C. H., and Yedidia, I. (2012) The role of secretion systems and small molecules in soft-rot *Enterobacteriaceae* pathogenicity, *Annu Rev Phytopathol* 50, 425-449.
- [18] Marquez-Villavicencio Mdel, P., Weber, B., Witherell, R. A., Willis, D. K., and Charkowski, A. O. (2011) The 3-hydroxy-2-butanone pathway is required for *Pectobacterium* carotovorum pathogenesis, *PLoS One* 6, e22974.
- [19] Grove, A., Kushwaha, A. K., and Nguyen, K. H. (2015) Determining the role of metal binding in protein cage assembly, *Methods Mol Biol* 1252, 91-100.
- [20] Sivapragasam, S., Pande, A., and Grove, A. (2015) A recommended workflow for DNase I footprinting using a capillary electrophoresis genetic analyzer, *Anal Biochem 481*, 1-3.
- [21] Perera, I. C., and Grove, A. (2011) MarR homologs with urate-binding signature, *Protein Sci* 20, 621-629.

- [22] Praillet, T., Reverchon, S., and Nasser, W. (1997) Mutual control of the PecS/PecM couple, two proteins regulating virulence-factor synthesis in *Erwinia chrysanthemi*, *Mol Microbiol* 24, 803-814.
- [23] Deochand, D. K., Perera, I. C., Crochet, R. B., Gilbert, N. C., Newcomer, M. E., and Grove, A. (2016) Histidine switch controlling pH-dependent protein folding and DNA binding in a transcription factor at the core of synthetic network devices, *Mol Biosyst* 12, 2417-2426.
- [24] Bordelon, T., Wilkinson, S. P., Grove, A., and Newcomer, M. E. (2006) The crystal structure of the transcriptional regulator HucR from *Deinococcus radiodurans* reveals a repressor preconfigured for DNA binding, *J Mol Biol 360*, 168-177.
- [25] Newberry, K. J., Fuangthong, M., Panmanee, W., Mongkolsuk, S., and Brennan, R. G. (2007) Structural mechanism of organic hydroperoxide induction of the transcription regulator OhrR, *Mol Cell* 28, 652-664.
- [26] Rohs, R., Jin, X., West, S. M., Joshi, R., Honig, B., and Mann, R. S. (2010) Origins of specificity in protein-DNA recognition, *Annu Rev Biochem* 79, 233-269.
- [27] Zhou, T., Yang, L., Lu, Y., Dror, I., Dantas Machado, A. C., Ghane, T., Di Felice, R., and Rohs, R. (2013) DNAshape: a method for the high-throughput prediction of DNA structural features on a genomic scale, *Nucleic Acids Res* 41, W56-62.
- [28] Fuangthong, M., and Helmann, J. D. (2002) The OhrR repressor senses organic hydroperoxides by reversible formation of a cysteine-sulfenic acid derivative, *Proc Natl Acad Sci U S A 99*, 6690-6695.

- [29] Birukou, I., Tonthat, N. K., Seo, S. M., Schindler, B. D., Kaatz, G. W., and Brennan, R. G. (2013) The molecular mechanisms of allosteric mutations impairing MepR repressor function in multidrug-resistant strains of *Staphylococcus aureus*, *MBio* 4, e00528-00513.
- [30] Crothers, D. M., Gartenberg, M. R., and Shrader, T. E. (1991) DNA bending in protein-DNA complexes, *Methods Enzymol* 208, 118-146.
- [31] Philips, S. J., Canalizo-Hernandez, M., Yildirim, I., Schatz, G. C., Mondragon, A., and O'Halloran, T. V. (2015) TRANSCRIPTION. Allosteric transcriptional regulation via changes in the overall topology of the core promoter, *Science* 349, 877-881.
- [32] Martell, D. J., Joshi, C. P., Gaballa, A., Santiago, A. G., Chen, T. Y., Jung, W., Helmann, J. D., and Chen, P. (2015) Metalloregulator CueR biases RNA polymerase's kinetic sampling of dead-end or open complex to repress or activate transcription, *Proc Natl Acad Sci U S A 112*, 13467-13472.
- [33] Rouanet, C., Reverchon, S., Rodionov, D. A., and Nasser, W. (2004) Definition of a consensus DNA-binding site for PecS, a global regulator of virulence gene expression in *Erwinia chrysanthemi* and identification of new members of the PecS regulon, *J Biol Chem* 279, 30158-30167.
- [34] Dorman, C. J., and Dorman, M. J. (2017) Control of virulence gene transcription by indirect readout in *Vibrio cholerae* and *Salmonella enterica* serovar Typhimurium, *Environ Microbiol* 19, 3834-3845.

- [35] Weinstein-Fischer, D., Elgrably-Weiss, M., and Altuvia, S. (2000) *Escherichia coli* response to hydrogen peroxide: a role for DNA supercoiling, topoisomerase I and Fis, *Mol Microbiol* 35, 1413-1420.
- [36] Griffiths, G. (2015) Biosynthesis and analysis of plant oxylipins, *Free Radic Res* 49, 565-582.
- [37] Price, M. N., Dehal, P. S., and Arkin, A. P. (2007) Orthologous transcription factors in bacteria have different functions and regulate different genes, *PLoS Comput Biol 3*, 1739-1750.